Available online at www.ilcpa.pl

International Letters of Chemistry, Physics and Astronomy

12 (2013) 82-93 ISSN 2299-3843

Enhanced photoelectrical performance of DSSC by Co-doped SnO_2 nanoparticles

C. Indira Priyadharsini[1], A. Prakasam[1], P. M. Anbarasan[1,2,*]

[1]Department of Physics, Periyar University, Salem - 636011, Tamil Nadu, India.

[2]Centre for Nanoscience & Nanotechnology, Periyar University, Salem - 636 011, Tamil Nadu, India

*Phone: +91-0427-2345766, 2345520, *Fax No: +91-0427-2345565, 2345124

*Email address: physicsprakasam@gmail.com

ABSTRACT

Investigation of the I-V characteristics of the DSSC based on interconnected with cobalt-doped SnO_2 nanoparticles covered with a nano-scale thin layer which was absorbed by natural dyes are described. The presence of co-doped SnO_2 has been confirmed by its characteristic XRD pattern and the shape of the particle is confirmed by SEM. The thickness of the protective layer can be conveniently controlled by the mole value of co-doped SnO_2 used in the preparation of the thin film and the optimum conditions for best performance of the DSSC are presented together with possible explanation for the variations observed. An optimum light-to-electricity conversion efficiency of 0.37 % in the presence of a layer of co-doped SnO_2 has been obtained which enhancement over the cell prepared with other natural dyes. The characterization of the sample using different techniques was explained (change the sentence).

***Keywords*:** co–doped SnO_2 nanoparticles; Natural Sensitizer; Structural properties; Absorption spectrum

1. INTRODUCTION

DSSC draws a quiet attention to meet future energy demand especially in the solar energy market demanding low cost photovoltaic devices. Low cost DSSCs, introduced by B. O'Regan et al. in 1991 have reached high solar to electric power conversion efficiency currently exceeding 11 % [1]. Efficiency of solar cells depends on its light harvest efficiency, the quantum yield for charge injection, and the charge collection efficiency at the electrodes [2]. The large internal surface area of the nanoparticles film, the light-harvesting efficiency of the dye monolayer is high, which means that one of the key components of DSSCs is the nanocrystalline semiconductor electrode. So far the highest energy conversion efficiencies have been achieved with nanocrystalline anatase TiO_2 [3,4]. Other materials, such as SnO_2 [5-8], ZnO [9-14], and Nb_2O_5 [15], have been tested as supports for dye molecules and electron transporting media, but their energy conversion efficiencies turn out to be mostly as

low as 1-2 %. For the case of SnO_2, it has been reported that almost all the excited dye molecules inject electrons on SnO_2 within ~150 ps [16], suggesting electron injection process does not seem to be responsible for considerably low energy conversion efficiency [17].

Organic dyes have often presented problems as well, such as complicated synthetic routes and low yields. Nonetheless, the natural dyes found in flowers, leaves, and fruits can be extracted by simple procedures. Due to their cost efficiency, non-toxicity, and complete biodegradation, natural dyes have been a popular subject of research. Thus far, several natural dyes have been utilized as sensitizers in DSSCs, such as cyanin [18-27], chlorophyll [28] etc. In this paper we investigate the effect of structural and morphology of SnO_2 nano particles on the performance of DSSC by comparing cells with different natural dyes.

2. EXPERIMENTAL

2. 1. Preparation of nanoparticles

Nanoparticles of Cu-La-SnO_2 were prepared by chemical co-precipitation method. For the synthesis of Co-doped SnO_2, two aqueous solutions were prepared according to the mole composition (0.03:0.0002:0.00003). Solution A containing: $SnCl_4 \cdot 5H_2O$, Solution B containing: $LaN_3O_9 \cdot 6H_2O$, $Cu(C_2H_3O_2)_2 \cdot 2H_2O$.

Deionised H_2O was added to solution B to increase its salts solubility. These solutions were mixed with constant stirring with magnetic stirrer. Then NH_4OH solution was added drop wise to the reaction mixture for precipitation. Finally resultant precipitates were washed several times with deionized water to remove the impurities. The product was dried in a hot air oven at a temperature of 373 K to remove water content and then annealed at a temperature of 480 °C for 3 h at ambient atmosphere to attain SnO_2 with improved crystallinity. To obtain the nanoparticles of La doped SnO_2 and pure SnO_2 the above procedure was followed.

2. 2. Preparation of Natural Sensitizer

Mature Tridax procumbens leaves, collected from a number of Tridax procumbens plants which obtained from botanical garden, Periyar University, Salem. Leaves were washed repeatedly with water to remove dust and soluble impurities and were allowed to dry first at room temperature in a shade and then in an air oven at 373 K for 1 h when the leaves became crisp. After being dried, the leaves were crushed in a mortar to make them into powder. About 1 g of the powdered sample was dissolved in 60ml of acetone and kept for two days at ambient temperature for adequate extraction without exposure to sunlight. After the extraction, the solid residues were filtered out, and the clear solutions were used as prepared, without purification. Further purification of the extracts was avoided so as to achieve efficient sensitization using simple extraction procedures. The extractants were properly stored, protected from direct sunlight, and used further as sensitizers in DSSCs. The same above procedure followed for the preparation of dyes from Rose leaves, Eclipta Alba leaves, Coccinia indica leaves. Then the extract fluids of all these four leaves were blended at the ratio of 1:1 to serve as a natural dye mixture.

2. 3. Fabrication of DSSC

The typical procedure of the paste making and DSSC assembling is followed to make the SnO_2 based DSSC. SnO_2 powder (300 mg), PEG (20 μl), acetic acid (160 μl) and ethanol

(2 ml) were mixed and ground well in order to obtain a paste. Doctor-bladed method was used to prepare a thin film of SnO_2 on FTO glass and it was sintered at 500 °C for 30 min. The photoelectrodes were soaked in a mixture of solution containing 0.3 mM natural dye in ethanol for 12 h at room temperature and then washed with ethanol and dried in air. Iodide/triiodide redox couple was used as an electrolyte.

2. 4. Characterization methods

Structural characterization was carried out by X-ray diffraction using Rigaku X-ray Diffractometer with CuKα radiation having wavelength λ = 1.5406 A˚ in the 2θ range from 20˚ to 80˚. The morphological features of the samples were also observed using the scanning electron microscope (SEM; Hitachi S-3000N). FT-IR spectroscopy measurements were carried out on a Bruker tensor 27 spectrophotometer using KBr pellets. PL experiments at room temperature were measured by using Fluoro Max-4. UV–VIS absorption spectra of natural dyes were recorded using a spectrophotometer Lamda 35.

3. RESULTS AND DISCUSSIONS

3. 1. Structural properties

The XRD pattern for all the synthesized samples are shown in Fig. 1 and it was observed that all the diffraction lines are assigned well to tetragonal rutile crystalline phase of tin oxide with a reference pattern (JCPDS 41-1445), and the diffraction peaks correspond to the (1 1 0), (1 0 1), and (2 0 0), (2 1 1), (2 2 0), (0 0 2), lattice plane respectively (doubt)s. Various parameter such as crystallite size (D), lattice constant (a) and cell volume (V), a/c ratio are calculated from the XRD data and their values are given in Table 1. Crystallite size of all samples is calculated using Scherer equation.1 [29,30].

$$k = \frac{\lambda}{\beta \cos\theta_B} \tag{1}$$

where 'K' is the Scherer's constant, 'λ' the wavelength of X-ray used, 'β' the full width at half maxima and 'θ' is the Bragg's angle. The average crystallite size was found in the range of 7.72-7.37 nm as shown in Table 1. The lattice constant (a) and cell volume (V) are calculated by the following equation (2, 3) [31, 32]

$$a=[d^2(h^2+k^2+l^2)]^{1/2} \tag{2}$$

$$V=a^2c \tag{3}$$

The intensity of pure SnO_2 nanoparticles decreases when compared to the rare earth & metal-doped SnO_2 nanoparticles. Consequently there was increase of crystallinity in the La and La-Cu-doped SnO_2 nanoparticles when compared to the pure SnO_2 nanoparticles. The ratio of the lattice parameters a and c is a measure of lattice distortion, it has been calculated from XRD data (Table 1).

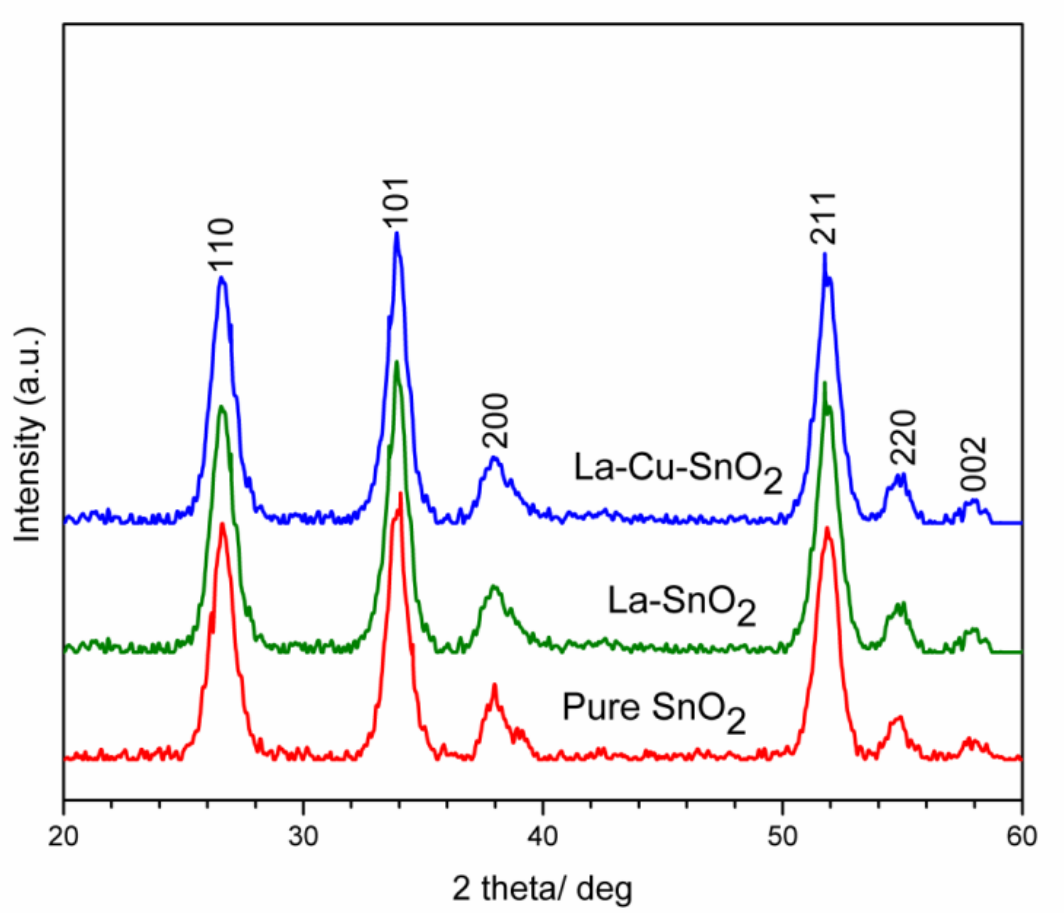

Fig. 1. XRD Analysis of Pure and Co Doped SnO_2 Nanoparticles.

Table 1. XRD Analysis of Pure & Co-doped SnO_2 Nanoparticles.

S.No.	Type of samples	Crystallite size (D) (nm)	Lattice Parameters (Å)	Cell Volume(V) ($Å^3$)	a/c ratio
1.	Pure-SnO_2	7.72	a = 4.751 c = 3.200	72.2304	1.4846
2.	La- SnO_2	7.46	a = 4.761 c = 3.200	72.5347	1.4878
3.	La-Cu- SnO_2	7.37	a = 4.761 c = 3.200	72.5347	1.4878

The a/c ratio appears as constant in all the samples which indicate that the lattice distortion is almost independent of dopants in our samples.

From the above discussions, it can be concluded that the narrowing of the XRD peaks of SnO_2 nanoparticles occurred not only by lattice distortions. The increase in lattice constant and cell volume may be also due to the larger ionic radii of the doped cation than Sn.

3. 2. Fourier Transform Infrared Spectroscopy

Fig. 2 shows the FTIR spectrum of undoped and doped tin oxide powder thermally treated at 480 °C. The absorption band at 3750 cm^{-1} due to various stretching vibrations of a residual alcohol, water & Sn O-H groups was observed [33]. The weak peak at 2923 cm^{-1} belongs to the stretching vibrations of C–H bonds.

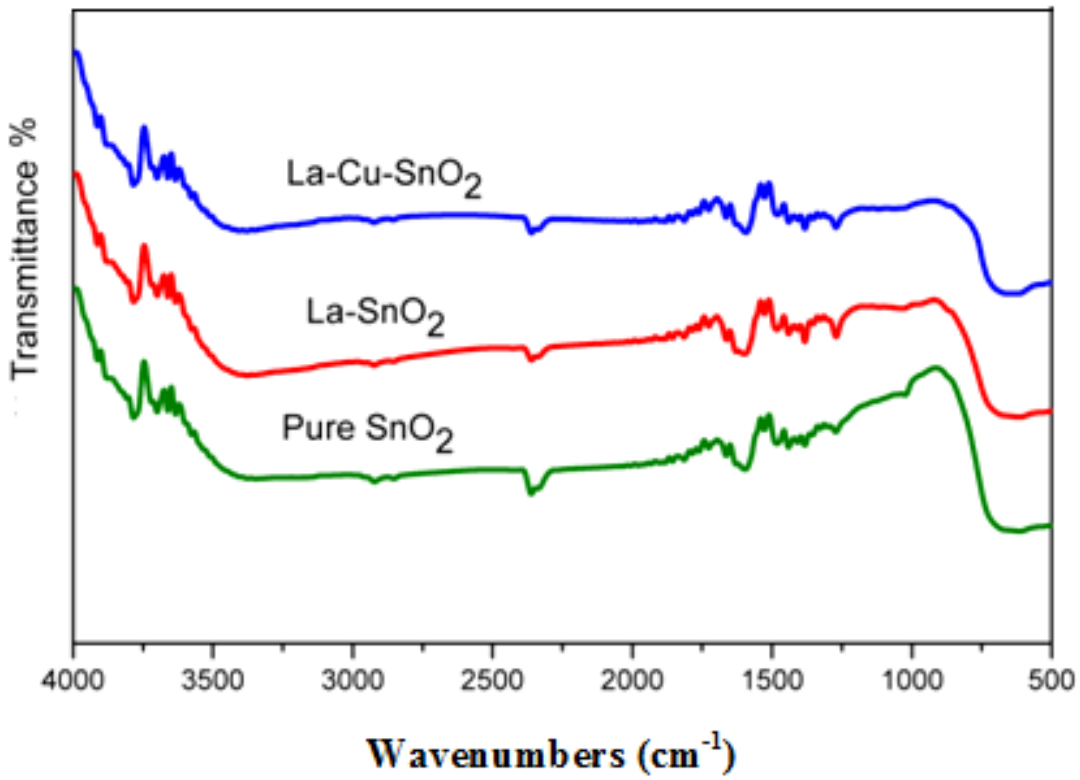

Fig. 2. FTIR analysis of Pure and Co doped SnO_2 nanoparticles.

The weak peak at 2361 cm^{-1} is probably due to the fact that the spectra were not recorded in situ and some absorption of H_2O or CO_2 from the ambient atmosphere has occurred [34].

The peak at 1600 cm^{-1} was attributed to presence of H_2O. The peak at 1441 cm^{-1} was assigned to the deformation of ammonia.

The broad band absorption at 613 cm^{-1} which is attributed to oxide-bridge functional group [35]. This elucidates the transformation of tin hydroxyl group to oxide group.

From the FTIR analysis it can be concluded that there were no affect in the peak while adding of dopants.

Table 2. FTIR analysis of Pure and Co-doped SnO_2 Nanoparticles.

Observed Frequency (cm^{-1})	Intensity	Assignment
3750	Strong	Stretching vibrations of OH
2923	Very weak	Stretching vibrations of –H
2361	Weak	Absorption of H_2O or CO_2
1600	Weak	Absorption of H_2O
1441	Very weak	Deformation of ammonia
613	Very strong	Oxide – bridge functional group

3. 3. Photoluminescence Spectroscopy

The optical properties of a semiconductor are related to both intrinsic and extrinsic effect. Photoluminescence spectroscopy is a suitable technique to determine the crystalline quality and the exaction fine structure. Fig 3 shows the PL spectrum corresponding to the excitation wavelength 425 & 450 nm respectively.

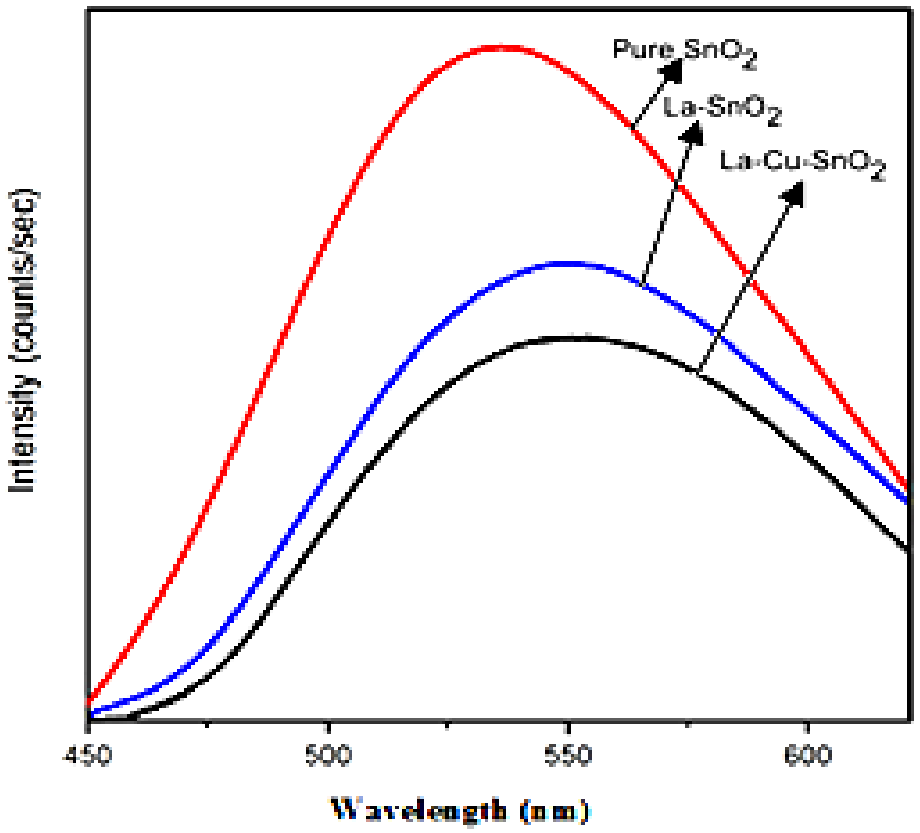

Fig. 3. Photolumincence Analysis of Pure and Co- Doped SnO_2 Nanoparticles.

The observed luminescence bands at 530 & 550 nm cannot be attributed to the direct recombination of a conduction electron in Sn 4d band with a hole in the O_2p valence band. Generally, defects such as oxygen vacancies are known to be the most common defects in tin oxides and usually act as radiative centers in luminescence process.

Broad luminescence bands between 500 & 600 nm can be explained due to defect levels in the band gap of SnO_2 nanoparticles at room temperature in agreement with earlier reports [36-40]. From the PL spectra it was absorbed that the intensity of the peaks decreases with adding of different dopants, at the same time wavelength also increases so there is a red shift. The red emission is due to electric dipole transition.

3. 4. Morphological Properties

Nano-SnO_2 is known to exhibit a large variety of morphologies with interesting size. Therefore, a growth control of the nanostructure has always been a critical issue. SEM micrographs of three samples with different morphology are shown in Fig. 4. From SEM analysis it can be observed that (Fig. (a)) are consist of large agglomerated pure SnO_2 nanoparticles. For La-doped SnO_2 nanoparticles (Fig. (b)) has a better dispersivity compared with the pure SnO_2, still a large agglomerated particles present in it. For La-Cu-doped SnO_2 nanoparticles (Fig. (c)), few agglomerated particles can be found, the particles are regular and looks like a square shape particles. From SEM analysis, it can be seen that the average crystallite size of the samples was acceptable agreement with XRD data.

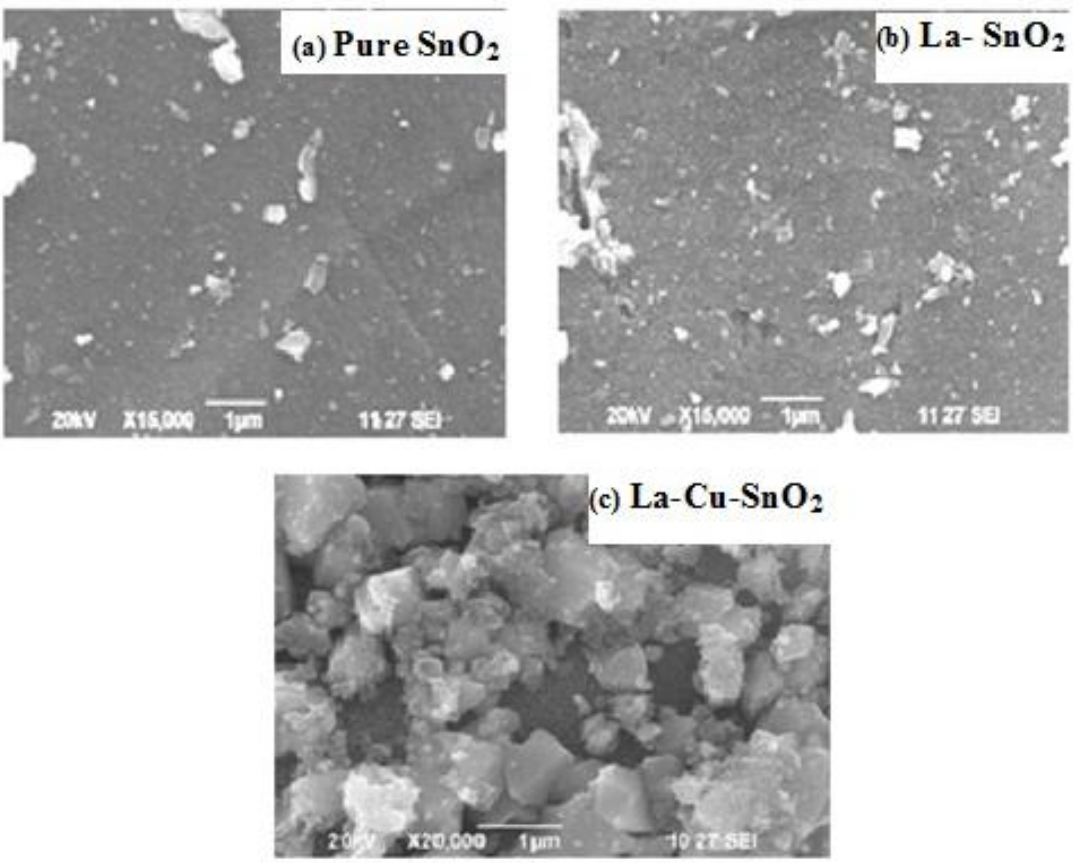

Fig. 4. SEM Analysis of Pure and Co Doped SnO_2 Nanoparticles.

3. 5. UV-VIS Analysis for Natural Sensitizer

Fig. 5 shows the absorption spectra in the region from 400 to 800 nm for the different types of natural extracts diluted in acetone. In this absorption spectra there is a peak presented at 400to 500 and 600 to 700 nm. But there is a first maximum peak at 400 to 500nm.In the case of wavelength maximum there is a difference in each leaves and mixing of extracts. Table 3 shows the maximum wavelength of different leaves.

Table 3. Wavelength Maximum of Different Natural Sensitizers.

S. No.	Leaf extract	λ_{max}
1	Eclipta alba	433
2	Coccinia indica	420
3	Tridax procumbens	421
4	Rosa lamella	358
5	Blend of above 4 leaves	404

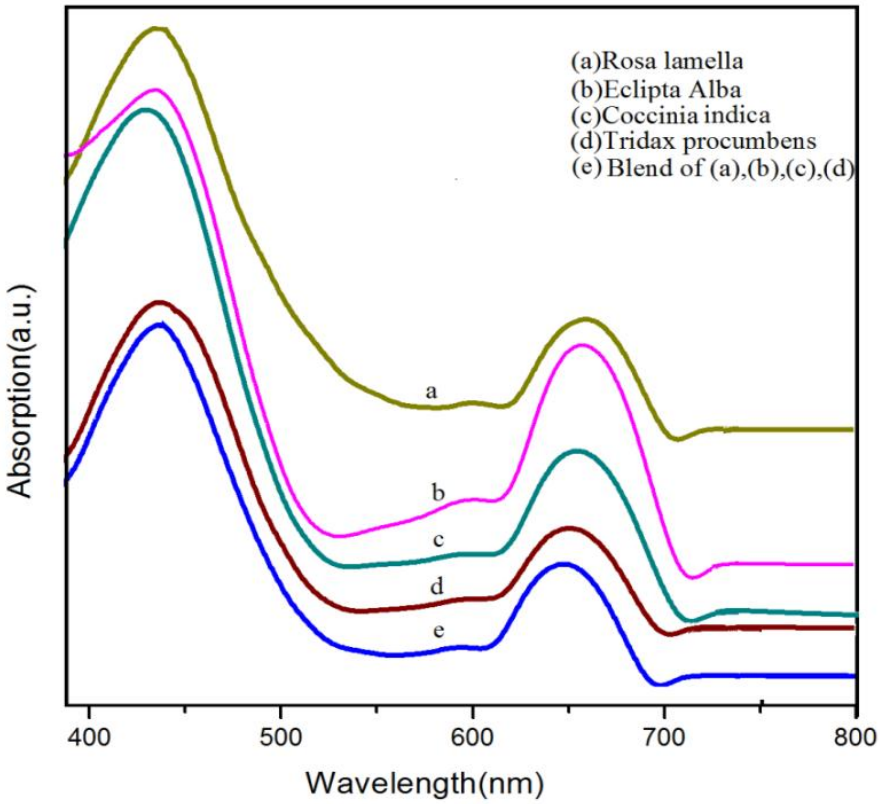

Fig. 5. UV-Vis analysis for Natural Sensitizers.

The absorption peak of chlorophyll exhibits red shift. Chlorophyll is a well known compound for photosynthesis. This UV-VIS absorption conforms that that leaf extract having chlorophyll.

3. 6. Characterisation of DSSC

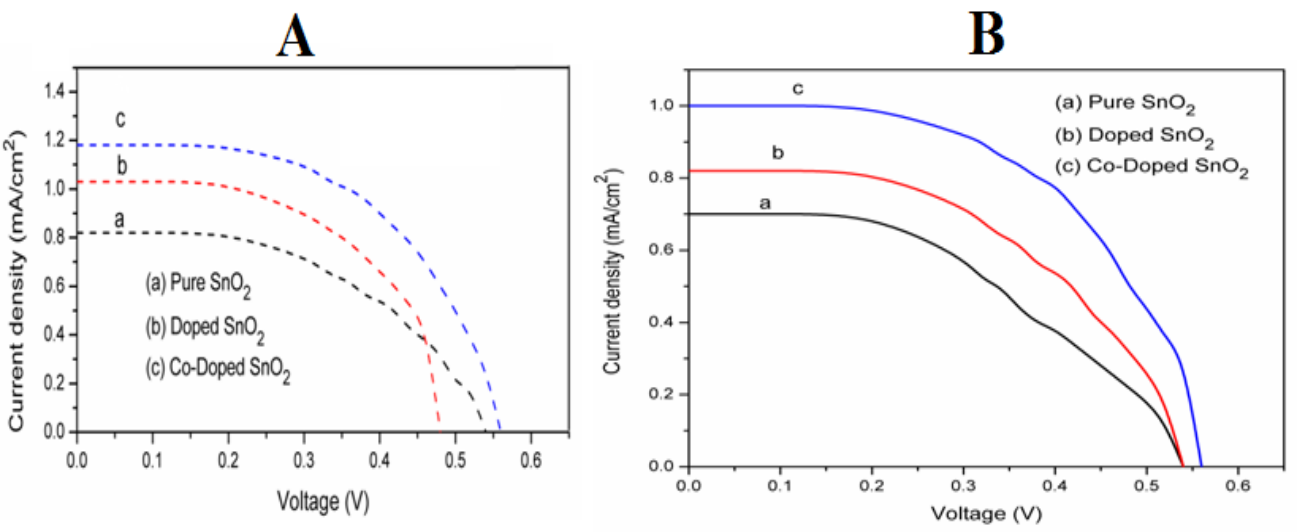

Fig. 6. I-V Characteristics Curve of (A) Cocinia Indica (B) Eclipta Alba.

Fig.7 shows the I–V (current–voltage) curve for the sunlight-illuminated of Eclipta Alba leaves, Coccinia Indica leaves extract sensitized cell. Table 4 presents the performance of the DSSCs in terms of short circuit photocurrent (I_{sc}), open-circuit voltage (V_{oc}), fill factor (FF) and energy conversion efficiency (η). It conclude that, using the Eclipta Alba leaf, have the best sensitization effect, under AM 1.5 illumination, reaching 0.37 % of solar energy conversion efficiency.

Table 4. I-V Characteristics Parameters.

Samples	Extracts	I_{sc}	V_{oc}	FF	(η) %
a) Pure SnO_2	Eclipta Alba	0.82	0. 4	0.54	0.29 %
b) Doped SnO_2		1.03	0.48	0.68	0.34 %
c) Co-Doped SnO_2		1.27	1.30	0.53%	0.37 %
a) Pure SnO_2	Cocinia Indica	0.7	0.54	0.61	0.26 %
b) Doped SnO_2		0.82	0.54	0.54	0.29 %
c) Co-Doped SnO_2		1.01	0.56	0.51	0.31 %

Obviously, natural dyes show sensitization activity lower than synthetic ones and less stability. The photoelectric conversion efficiency of Eclipta Alba leaf extract fluid is higher than the photoelectric conversion efficiency of Coccinia Indica, leaves extract fluid.

This is because, after the Eclipta Alba leaf extract is adsorbed on the surface of SnO_2 nanoparticles, the absorption intensity is higher and the absorption wavelength range is broader than those after the Coccinia indica, leaves extract is adsorbed on the surface of SnO_2 nanoparticles. In addition, there is a higher interaction between SnO_2 nanoparticles and the chlorophyll in Eclipta Alba leaf extract fluid, giving the produced DSSCs better charge-transfer performance, clearly improved efficiency. The reason was that the electrons can be transported from excited Eclipta Alba leaf extract dyes molecule to SnO_2 thin film was much higher than the excited Coccinia indica, leaves extract dyes molecule to SnO_2 thin film.

4. CONCLUSION

DSSCs are photoelectrochemical solar devices, currently subject of intense research in the framework of renewable energies as a low-cost photovoltaic device. Their functioning is based on the interlacing of subsystems working in tandem: the photoanode on which the dye sensitizer is adsorbed, the electron mediator and the counter electrode. Pure and Co-doped SnO_2 nanoparticles were prepared by chemical co-precipitation method.

1) Finely prepared SnO_2 nanoparticles having the crystallite size of 7.37-7.72 nm through XRD analysis.
2) From FTIR analysis it confirmed that the presence of oxide groups shows the formation of SnO_2.
3) Photoluminescence spectrum reveals that there is a red shift. So it can be conclude that there was a decrease of band gap.
4) From SEM analysis regular and square like particles are formed.
5) UV-VIS absorption spectrum confirms the presence of chlorophyll in the extracts.

The photoelectrical performance of the DSSCs based on Co-doped SnO_2 nanoparticles sensitized with Eclipta Alba dye having maximum efficiency of 0.37 % among the all sensitizers.

References

[1] M. K. Nazeeruddin, P. Péchy, T. Renouard, S. M. Zakeeruddin, R. Humphry-Baker, P. Comte, P. Liska, L. Cevey, E. Costa, V. Shklover, L. Spiccia, G. B. Deacon, C. A. Bignozzi, M. Grätzel, *Journal of the American Chemical Society* 123 (2001) 1613.
[2] M. Grätzel, Journal of Photochemistry and Photobiology A: Chemistry 164 (2004) 3.
[3] M. K. Nazeeruddin, A. Kay, I. Rodicio, R. Humphry-Baker, E. Muller, P. Liska, N. Vlachopoulos, M. Grätzel, *J. Am. Chem. Soc.* 115 (1993) 6382.
[4] M. K. Nazeeruddin, P. Pechy, T. Renouard, S. M. Zakeeruddin, R. Humphry-Baker, P. Comte, P. Liska, L. Cevey, E. Costa, V. Shklover, L. Spiccia, G. B. Deacon, C. A. Bignozzi, M. Grätzel, *J. Am. Chem. Soc.* 123 (2001) 1613.
[5] I. Bedja, S. Hotchandani, P. V. Kamat, *J. Phys Chem.* 98 (1994) 4133.
[6] S. Ferrere, A. Zaban, B. A. Gregg, *J. Phys. Chem.* B 101 (1997) 4490.

[7] F. Fungo, L. Otero, E. N. Durantini, J. J. Silber, L. E. Sereno, *J. Phys. Chem.* B 104 (2000) 7644.
[8] S. Chappel, A. Zaban, *Sol. Energy Mater. Sol. Cells* 71 (2002) 141.
[9] H. Rensmo, K. Keis, H. Lindström, S. Södergren, A. Solbrand, Hagfeldt, S.-E. Lindquist, L.N. Wang, M. Muhammed, *J. Phys. Chem.* B 101 (1997) 2598.
[10] K. Keis, J. Lindgren, S.-E. Lindquist, A. Hagfeldt, *Langmuir* 16 (2000) 4688.
[11] B. O'Regan, D. T. Schwartz, S. M. Zakeeruddin, M. Gratzel, *Adv. Mater.* 12 (2000) 1263.
[12] K. Hara, T. Horiguchi, T. Kinoshita, K. Sayama, H. Sugihara, H. Arakawa, *Sol. Energy Mater. Sol. Cells* 64 (2000) 115.
[13] C. Bauer, G. Boschloo, E. Mukhtar, A. Hagfeldt, *J. Phys. Chem.* B 105 (2001) 5585.
[14] K. Keis, E. Magnusson, H. Lindström, S.-E. Lindquist, A. Hagfeldt, *Sol. Energy Mater. Sol. Cells* 73 (2002) 51.
[15] F. Lenzmann, J. Krueger, S. Burnside, K. Brooks, M. Gratzel, D.Gal, S. Ruhle, D. Cahen, J. Phys. Chem. B 105 (2001) 6347.
[16] G. Benkö, P. Myllyperkiö, J. Pan, A. P. Yartsev, V. Sundström, *J. Am. Chem. Soc.* 125 (2003) 1118.
[17] Nam-Gyu Park, Man Gu Kang, Kwang Sun Ryu, Kwang Man Kim, Soon Ho Chang *Journal of Photochemistry and Photobiology A: Chemistry* xxx (2003) xxx–xxx
[18] P. M. Sirimanne, M. K. I. Senevirathna, E. V. A. Premalal, P. K. D. D. P. Pitigala, V. Sivakumar, K. Tennakone, *J. Photochem. Photobiol.* A 177 (2006) 324-327.
[19] S. Hao, J. Wu, Y. Huang, J. Lin, *Sol. Energy* 80 (2006) 209-214.
[20] A. S. Polo, N. Y. Murakami Iha, *Sol. Energ. Mat. Sol. Cell* 90 (2006) 1936-1944.
[21] K. Tennakone, A. R. Kumarasinghe, G. R. R. A. Kumara, K. G. U. Wijayantha, P. M. Sirimanne, *J. Photochem. Photobiol.* A 108 (1997) 193-195.
[22] D. Zhang, S. M. Lanier, J. A. Downing, J. L. Avent, J. Lumc, J. L. McHale, *J. Photochem. Photobiol.* A 195 (2008)72-80.
[23] J. M. R. C. Fernando, G. K. R. Senadeera, *Curr. Sci.* 95 (2008) 663-666.
[24] Q. Dai, J. Rabani, *J. Photochem. Photobiol*. A 148 (2002) 17-24.
[25] N. J. Cherepy, G. P. Smestad, M. Grätzel, J. Z. Zhang, *J. Phys. Chem.* B 101 (1997) 9342-9351.
[26] P. Luo, H. Niu, G. Zheng, X. Bai, M. Zhang, W. Wang, From salmon pink to blue natural sensitizers for solar cells: Canna indica L., *Spectrochim. Acta* Part A 74 (2009) 936-942.
[27] S. Furukawa, H. Iino, T. Iwamoto, K. Kukita, S. Yamauchi, *Solid Films* 518 (2009) 526-529.
[28] G. R. A. Kumara, S. Kaneko, M. Okuya, B. Onwona-Agyeman, A. Konno, K. Tennakone, *Sol. Energ. Mat. Sol.* C 90 (2006) 1220-1226.
[29] M. J. Iqbal, S. Farooq, *Mater. Sci. Eng.* B 136 (2007) 140.
[30] M. J. Iqbal, M. R. Siddiquah, *J. Alloys Compd.* 453 (2008) 513.
[31] I. H. Gul, F. Amin, A. Z. Abbasi, M. A. Rehman, A. Maqsood, *J. Magn. Magn. Mater.* 311 (2007) 494.
[32] A. A. Sattar, H. M. El-Sayed, W. R. Agami, A. A. Ghani, *J. Appl. Sci.* 4 (2007) 89.
[33] Pietro Siciliano Sensors and Actuators B 70_2000.153-164.
[34] J. Jouhannaud, J. Rossignol, D. Stuerga, *Journal Of Solid State Chemistry* 181(2008) 1439-1444.
[35] T. Krishna Kumar, R. Jayaprakash, M. Parthibavarman, A. R. Phani, V. N. Singh, B. R. Mehta, *Materials Letter* 63 (2009) 896-898.

[36] Hu J. Q., Ma X. L., Shang N. G., Xie Z. Y., Wong N. B., Lee C. S., Large scale rapid oxidation synthesis of SnO_2 nanoribbons.
[37] Hu J. Q., Bando Y., Liu Ql, Golberg D., *Adv. Functional Matter* 13 (2003) 493-6.
[38] Calestani D., Lazzarini L., Salvaiti G., Zha M., *Cryst. Res. Technol.* 40 (2005) 937-41.
[39] Fagila G., Baratto C., Sberveglieri G., Zha M., Zappettini A., *Appl. Phys. Lett.* 86 (2005) 01923.
[40] Mastre D., Cremades A., Piqueras J., *J. Appl. Phys.* 97 (2015) 044316.

(Received 13 August 2013; accepted 16 August 2013)